

# THE AUTOMATIC EXTRACTION OF DEM DATA FROM STEREO RADARSAT PAIRS OVER THE TROPICS

Andrew Sowter, Chief Radargrammetrist

National Remote Sensing Centre Limited, Delta House, Southwood Crescent, Southwood, Farnborough, UK

Commission II, Working Group 6

**KEYWORDS:** Stereo, SAR, DEM, Radarsat, Radargrammetry

## ABSTRACT

Stereo SAR has been around for many years but only recently has the global supply of stereo pairs been available through the Canadian Radarsat satellite. This paper explores the potential exploitation of the technique for the generation of coarse but low-cost DEMs over the tropics. A number of sites around the Lake Kutubu area in Central Papua New Guinea were selected and DEMs derived using a completely automated process from Radarsat Standard Mode data. The results demonstrate the feasibility of the technique for low to moderate relief; in more rugged terrain, the use of Radarsat Fine Mode data is recommended to reduce the effect of extreme foreshortening and layover on the output quality.

## 1. BACKGROUND

### 1.1 Introduction

SAR is well known as a provider of remote sensing data in cloud-free areas and has been routinely used in the tropics for over 30 years, primarily to provide geological information to the commercial oil and gas exploration industry (e.g. Graham, 1980). To identify or derive topographic data is also problematic over those areas and reliance has generally been placed on the identification of maps, where possible, albeit of variable quality and age. Aerial photography is generally poor over the region due to cloud but also because any blanket coverage of rainforest will mask the topography to some extent. SAR, on the other hand, highlights the topography and therefore should be a good source of such data.

Little stereo SAR data has been available from aerial and spaceborne sensors until very recently. The main reason for this is that most antennas have had fixed elevation angles (the angle from Nadir) and therefore the only source of stereo has been from opposite side or overlapping pairs (Leberl, 1980), which are not the most easy (in the first case) or the most accurate (in the latter) cases to use. Even ERS-1 and -2 have fixed elevation angles, although the ERS-1 satellite was physically steered to increase the elevation angle from approximately  $23^\circ$  to  $35^\circ$  for one month during a "Roll-Tilt" Mode.

In 1995, the Canadian Radarsat satellite was launched as a commercial provider of stereo SAR data worldwide (RSI, 1995). Uniquely amongst commercial satellites, Radarsat has a steerable antenna and is therefore able to view from elevation angles between  $20^\circ$  and  $50^\circ$ . The configuration of the satellite and its ground segment means that good quality stereo data should be available anywhere in the world, acquired to order.

Thus, there is now an opportunity to provide topographic data quickly and cheaply to anyone who requires it. The imminent launch of the European ENVISAT satellite which has a similar capability (ESA, 1997) and after this, Radarsat-2, means that the availability of such data will be guaranteed for years to come.

## 2.2 Principles

The Stereo SAR technique is very well understood, obviously deriving from the corresponding optical technique but with some refinements to use radargrammetric, as opposed to photogrammetric, principles. Radar is very different to optical in the way that data is organised and most successful methods use a radar methodology. However, good approximations can be made by approximating a photogrammetric model, especially over small areas, which are computationally more efficient.

The basis of any stereo process is that, by looking at the same point from two different positions in space, we can calculate the full 3-d position of that point. This is illustrated below in Figure 1.

In Figure 1, the target is imaged from a sensor at two different positions in orbit, given by the position vectors  $P_1$  and  $P_2$  related to the origin of the Earth at  $O$ . In radar, the important geometrical parameters are the value of the Doppler Centroid, which gives the look angle, and the slant range, which is the distance from the sensor to the target, given here as values  $R_1$  and  $R_2$  in the figure. From these parameters, and an orbit model, it is possible to derive the three-dimensional position vector of the target point,  $P_T$ .

Using standard geodetic equations, the 3-d position vector  $P_T$  can be transformed into map coordinates (e.g. Northings and Eastings) and a height above a reference ellipsoid or geoid. When arranged into a regular map coordinate grid, the heights are referred to as a digital elevation model (DEM).

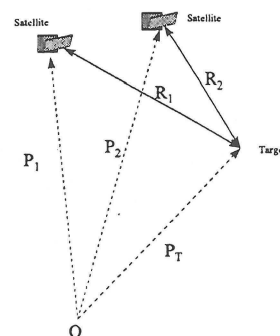


Figure 1. The Radar Stereo Principle.

Thus, starting with a suitable image pair, it is possible to systematically identify the same points in each image and then derive their coordinates. This process involves:

- **Stereo Matching** - systematically identifying the same point in the two different images.
- **Intersection** - calculating the ground coordinates (position and height) for every matched point.

Methods of stereo matching are various, ranging from completely manual pixel-by-pixel matching, which is very slow and expensive, through to a completely automated technique based on image-to-image correlation. Clearly, the latter is most attractive from a cost point of view although it may not always yield the most accurate result.

Intersection is a very well-defined problem and has been approached through photogrammetric modelling (Toutin and Carboneau, 1992) and, more appropriately through radargrammetric modelling (Dowman et al., 1997).

Stereo SAR pairs can, by definition, only be approached by two schemes, same side and opposite side, due to the side-looking nature of the instrument. This is illustrated in Figure 2 below.

Opposite side views give by far the greater accuracy, having the greatest disparity between the two views. However, the views look completely different and can only be matched using a mostly manual process which is time consuming and expensive.

Same side views are much easier to match automatically, looking very much the same, and so are much easier and quicker to process, although at the cost of accuracy.

### 2.3 Accuracy

The geometric accuracy of any stereo information derived from any source depends on two factors:

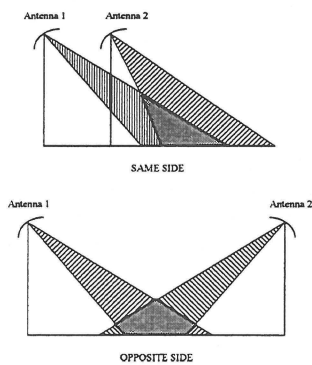


Figure 2. Basic Orbit Configuration for Stereo SAR

**Localisation.** This relates to the positional accuracy of the data (i.e. how accurately it can be located on the Earth's surface) and is generally dependent on the accuracy of a number of parameters such as image timing, orbit accuracy, image processing etc.

**Spatial Resolution.** This relates to our ability to distinguish two separate targets within an image. The spatial resolution is defined as the minimum distance two targets have to be

apart in order for us to be able to say, with confidence, that they are, indeed, two targets.

For a stereo-derived product, both factors influence the final accuracy. In terms of localisation, relating to the positional accuracy of heights or pixels, the accuracy is variable. For Radarsat data, this information is not readily available but is anticipated to be better than 500m without ground control. Obviously, if ground control points (GCP's) are available, then the localisation accuracy can be improved to the order of the spatial resolution which, for Standard Mode data is 30m.

The height accuracy is wholly dependent on the spatial resolution and the difference in look angle between the stereo views. Consider the same-side viewing configuration illustrated in Figure 3 below where we have a target at height  $h$  viewed at incidence angles  $\theta_1$  and  $\theta_2$  respectively.

From simple trigonometry, we can show that the displacement of the target from its true position when viewed from Position 1, caused by the foreshortening effect of the radar, is given by  $x_1$  where:

$$x_1 = h \cot \theta_1$$

Similarly, the displacement caused by viewing from Position 2 is given by  $x_2$  where

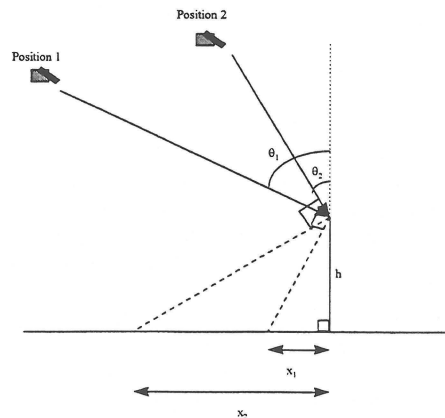


Figure 3. Same Side Stereo SAR Geometry

$$x_2 = h \cot \theta_2$$

If we are to gain stereo information from the two views, the only condition is that the difference in displacement caused by viewing from the two positions is measurable. This means, simply, that:

$$|x_2 - x_1| \geq \rho$$

where  $\rho$  is the spatial resolution of the image.

We can easily invert this equation to find the minimum height difference measurable from stereo SAR for any given spatial resolution and incidence angle combination. This is:

$$H = \rho / (\cot \theta_2 - \cot \theta_1)$$

where  $H$  is the minimum height resolvable.

Below, the value of  $H$  is calculated for a number of representative combinations of Radarsat and ERS data, assuming same side geometry.

Combination	Angular Range (degrees)	H (metres)
ERS PRI Near and Far Range	19-26	35.1
Radarsat S1 and S7	23-47	21.1
Radarsat S2 and S7	27-47	29.1
Radarsat F1 and F5	38-47	25.5

Table 1. Minimum Height Resolvable from Various SAR Image Combinations.

The value of  $H$  shown in the table is effectively the relative height accuracy of a stereo SAR-derived DEM.

### 1.3 Summary

In theory at least, stereo SAR is a potentially good source of medium resolution DEM and image data giving accuracies to as good as 30m in all directions. The current availability of stereo SAR data means that such topographic data is now routinely available over any part of the tropics. Such coverage has never been available before and therefore the time is ripe to exploit this information.

The commercial exploitation of stereo SAR will be determined by its accuracy in some cases but on the whole the cost of buying the remotely sensed data and extracting the information must not counterbalance the technical benefits. With Radarsat data, the image costs are already high, meaning that some \$6000-\$8000 is needed for the data alone. Thus, in order to gain market placement, a low-cost DEM extraction methodology must be employed.

At NRSC, a fully automated DEM and Ortho-Image generation algorithm has been prototyped to demonstrate a low cost stereo SAR methodology. This paper will demonstrate the results of using the prototype over an area of interest to the oil and gas industry and conclude of the usefulness of the products for exploitation of this widely available source of data.

## 2. SITE AND DATA DESCRIPTION

### 2.1 The PNG Site

The site chosen for this study was the area surrounding Lake Kutubu in Central Papua New Guinea (PNG). The Lake is situated at approximately 143° 20'E and 6° 25'S in the Southern part of the Central Range of mountains. An outline of its location is shown in Figure 4.

The lake itself is situated approximately 800m above mean sea level and is surrounded by terrain which is totally covered by dense tropical rain forest. It is a site of ongoing exploration for non-renewable resources and there are a number of well sites in the area, particularly in the anticline structure along most of the South West shore of the lake. At the top of the lake, just to the West is an airstrip (the Mora Landing Strip).



Figure 4. The Location of the Lake Kutubu Site

Away from the lake and to the North, the terrain becomes more severe with some peaks having altitudes of around 3000m. In the immediate vicinity of the lake there are a few flat swampland areas but as we move to the South West the topography is undulating in folds that rise up to around 1400m at most, dying away as they reach the large flat Karstified region of the Great Papuan Plateau.

### 2.2 The SAR Data

For the stereo analysis, two Radarsat demonstration images of the site were kindly provided by Radarsat International. Their details are given in Table 2 below.

	Image 1	Image 2
Scene Date	6 September 1996	9 September 1996
Scene Time	08:44:27.058 GMT	08:56:56.695 GMT
Beam Mode	Standard 2	Standard 7
Orbit	4384 - Ascending	4427 - Ascending
Product Type	Path Image	Path Image
Product Size	8207 lines x 9034 pixels	8112 lines x 8940 pixels
Pixel Spacing	12.5m	12.5m
Incidence Angle	27.633 degs	46.952 degs

Table 2. Radarsat Data Characteristics.

Imagettes of the two SAR scenes are shown below in Figures 5 and 6. Lake Kutubu stands out very clearly as the large dark feature in the centre of each. In each case, the scene is illuminated from the left of the image, causing the slope oriented to the left to be brighter than those oriented to the right. Note the difference in foreshortening characteristics between the two images (i.e. the extent to which the mountains seem to 'lean over' to the left), caused by the difference in incidence angle.

### 2.3 Map Sheets

For validation of the exercise, it was important to have an independent source of topographic data. Over many areas of the tropics, data at a scale suitable for this task may not be so readily available. For this site, however, we were fortunate enough to have a set of 1:100 000 topographic maps produced by the Royal Australian Survey Corps. The maps were first printed in 1974 and were produced using airborne

stereophotogrammetric methods. A description of the map quality and projection data is shown below in Table 3.

Accuracy	+/- 48m (x-y) , +/- 20m (z)
Scale	1:100 000
Contour Interval	40m
Horizontal Datum	Australian Geodetic Datum 1966
Vertical Datum	Mean Sea Level
Projection	Transverse Mercator (UTM Zone 54 South)
Size of Each Sheet	55km x 55km

Table 3. Map Sheet Parameters

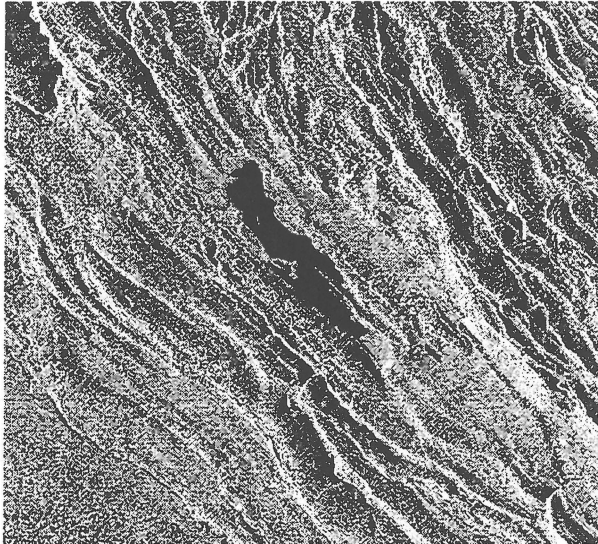


Figure 5. The Standard 2 Image of the Site.



Figure 6. The Standard 7 Image of the Site.

### 3. GENERATION OF THE DEM DATA

#### 3.1 Test Site Locations

As described in the previous section, the Lake Kutubu site contains great variations in types of topography. Therefore, it

is important to address the success of the stereo SAR in extracting information over all of the possible sites. To this end, three specific sites have been identified that contain topography of different characteristics:

- Site 1: Relatively flat area in the bottom left corner of the image.
- Site 2: Moderately undulating topography on the South West shore of the Lake.
- Site 3: Mountainous topography in the top right of the image.

The location of these sites is shown in Figure 7.

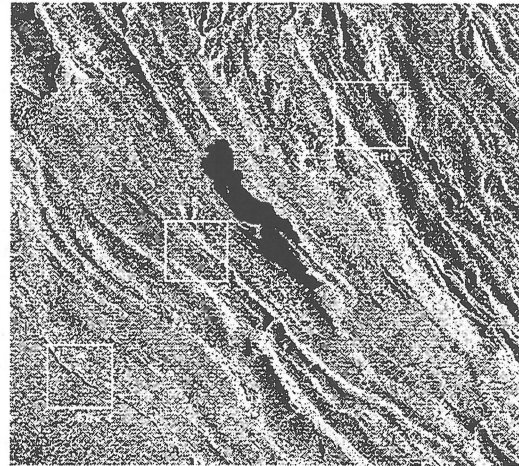


Figure 7. Location of the 3 Sites.

#### 3.2 Site 1 Analysis

Images of Site 1 are shown in Figure 8 below.

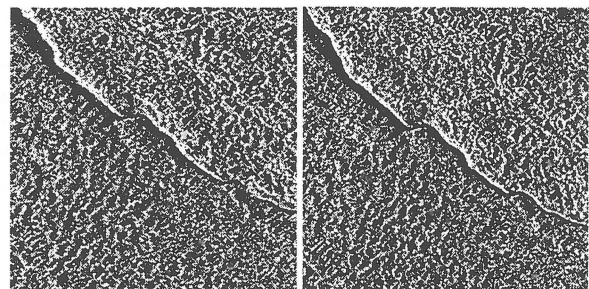


Figure 8. Standard 2 (left) and Standard 7 (right) Images of Site 1.

As is clear from the figure, very few features are apparent at this site, apart from the Hegigio River which runs from top left to bottom right. The texture away from the river is due to the numerous sinkholes and limestone pinnacles formed by the karsts.

The DEM and ortho-image generated by the stereo software are presented in Figure 9 below. Both are rectified to UTM Zone 54 South using the Australian National Datum as reference. All heights derived by the stereo analysis are referenced to the ellipsoid specified by the Australian Geodetic Datum 1966.

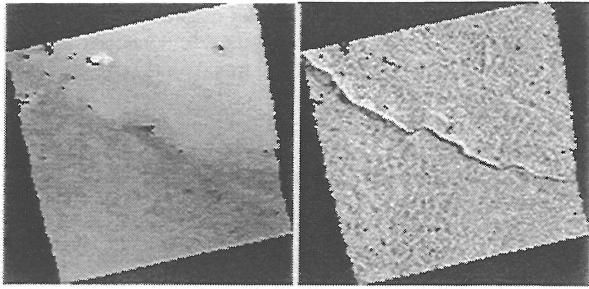


Figure 9. DEM (left) and Ortho Image (right) of Site 1.

From a qualitative point of view, the results successfully represent the area in question in that, except for a few obvious and isolated blunders, the relative flatness of the area is preserved. The river does have some influence on the DEM, forming a boundary between the Great Papuan Plateau in the south and the beginnings of some less karstified areas in the North.

A rendered 3-d view of the surface illustrates further the relative flatness of the terrain and is shown in Figure 10 below where the valley carved by the river is made much more apparent.

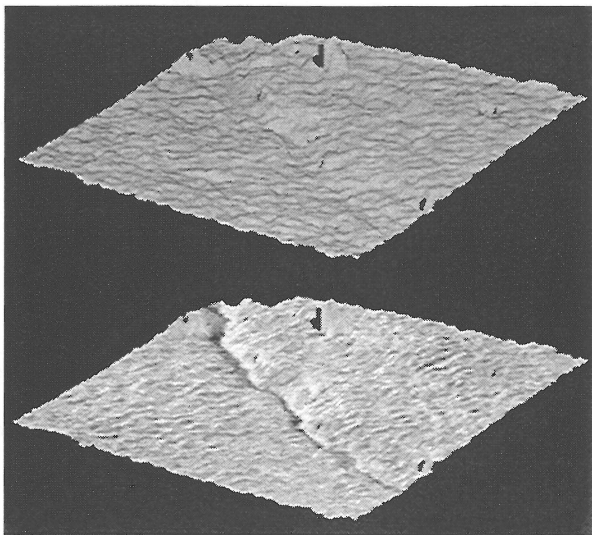


Figure 10. The DEM (top) and Image (bottom) viewed from the South West.

Profiles of the topography running North-South and West-East are shown in Figures 11 and 12. The river does cut out a noticeable canyon which is some 100m below the level of the plateau area which has a mean height of around 300m. To the North East of the river, the topography does rise slowly, reaching heights of around 600m. The main variations in topography in the plateau region are due to the sinkholes and pinnacles consistent with the karstification process. Comparisons with the profiles from the maps are generally excellent although it is difficult to gain any quantitative evidence due to the coarseness of the maps, where contours are given at 40m intervals.

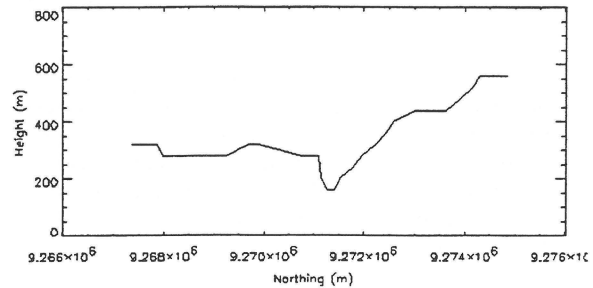
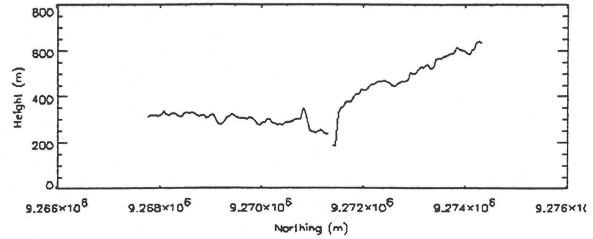


Figure 11. South-to-North Profiles from the Stereo-derived DEM (top) and the Maps (bottom)

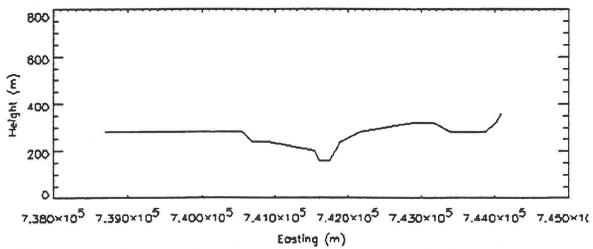
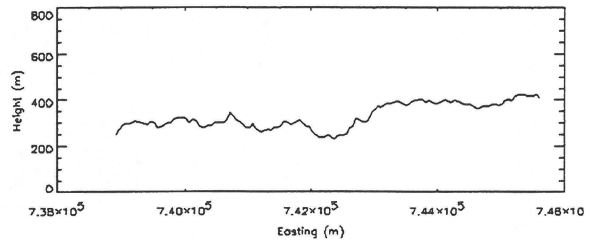


Figure 11. East-to-West Profiles from the Stereo-derived DEM (top) and the Maps (bottom)

The quantitative agreement between the profiles is very encouraging as the DEM was derived with no ground control at all. This confirms the validity of the radargrammetric model used and the unique orbit correction applied by the prototype. This correction is a unique feature of the software and is necessary due to the poor description of the orbit in Radarsat products.

### 3.3 Site 2 Analysis

Images of Site 2 are shown in Figure 12 below.

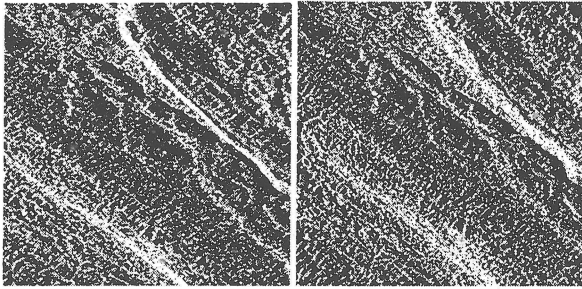


Figure 12. Standard 2 (left) and Standard 7 (right) Images of Site 2.

The image as shown is dominated by bright and dark tones caused by the illumination of the topography by the radar from the left side. There are two ridges in the image running from middle top to middle right and from middle left to middle bottom, respectively. Few other features of note exist, apart from the Digimu River which runs from approximate top left to middle right, as, again, the land is totally covered in tropical forest.

The DEM and ortho-image generated by the stereo software are presented in Figure 13 below.

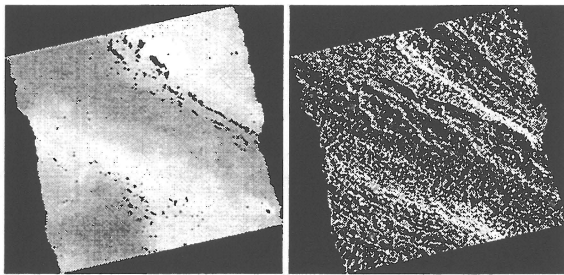


Figure 13. DEM (left) and Ortho Image (right) of Site 2.

From a qualitative point of view, the results successfully represent the area in question in that, except for a few obvious and isolated blunders, the presence of the two ridges either side of the river are preserved.

A rendered 3-d view of the surface illustrates further the influence of the two ridges is shown in Figure 14 and also shows more clearly the path carved by the river.

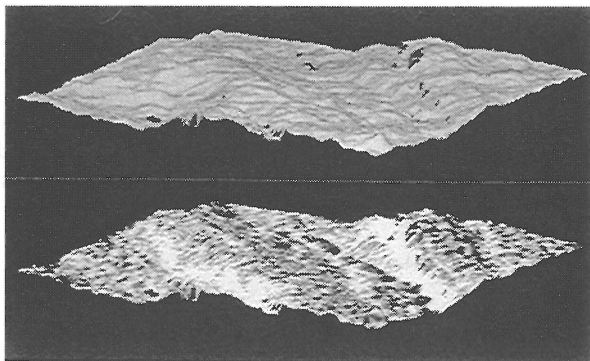


Figure 14. The DEM (top) and Image (bottom) viewed from the South West.

Profiles of the topography running North-South and West-East are shown in Figures 15 and Figure 16. Qualitatively, there is good agreement with the general trends in the topography along both profiles although there are some areas of disagreement, specifically at the beginning of the North-South profile, where the dip in the DEM is not as great as that from the maps, and the canyon seen at the end of the East-West profile in the map but not in the DEM.

Quantitatively, there is also excellent agreement between the profiles, demonstrating again the validity of the geometric model used within the intersection.

Both profiles illustrate the problem that the stereo matching has in areas of foreshortening. The front of a slope appears very different in two stereo pairs and is very hard to match properly. In this case, this is compounded by a poor match either side of the slope which causes any steepness to be flattened out.

However, this is not seen all over the DEM and is mainly isolated to the southernmost part of the image in general. The problem along the river canyon is also an illustration of this effect.

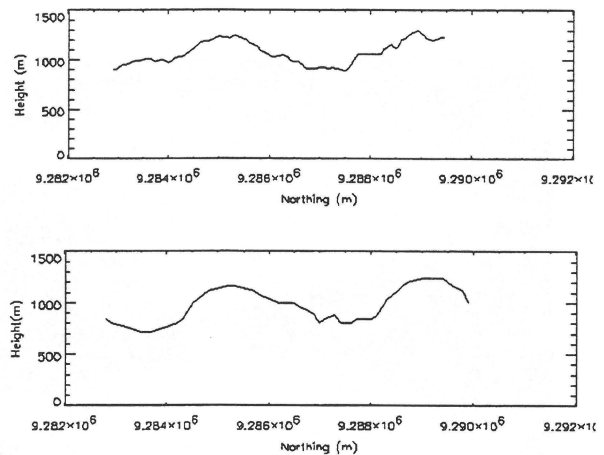


Figure 15. South-to-North Profiles from the Stereo-derived DEM (top) and the Maps (bottom)

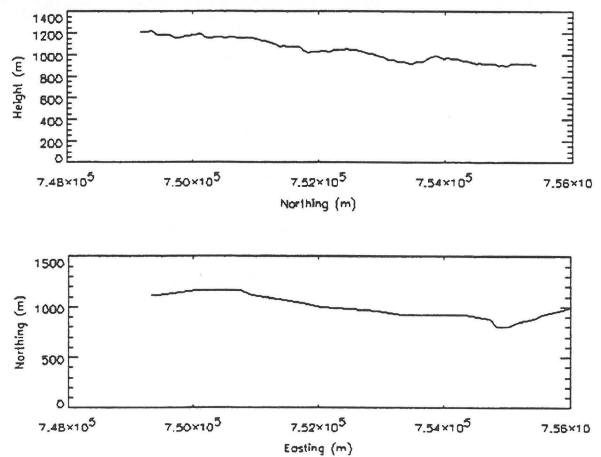


Figure 16. East-to-West Profiles from the Stereo-derived DEM (top) and the Maps (bottom)

### 3.4 Site 3 Analysis

Images of Site 3 are shown in Figure 17 below.

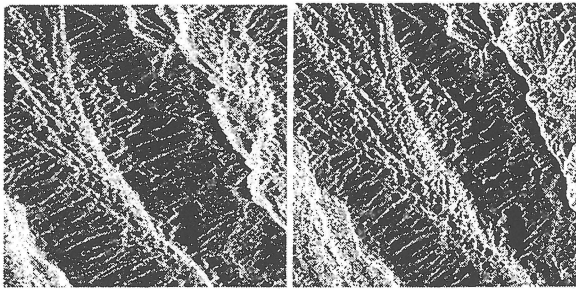


Figure 17. Standard 2 (left) and Standard 7 (right) Images of Site 3.

The site is composed of a number of valleys separated by ridges. This particular location is subject to sufficiently severe terrain variations resulting in areas of layover and shadow. From Figure 17, there are areas of shadow apparent on the right side of the top-left-to-bottom-right ridge. There is also a very foreshortened region to the right of the canyon formed by the Waga River (right of image). In the Standard 2 image, this is subject to layover which almost wholly obscures the river completely.

The DEM and ortho-image generated by the stereo software are presented in Figure 18 below. The stereo analysis has preserved the valley-ridge make-up of the site and, qualitatively at least, the results are successful. When comparing the ortho-image to Figure 17, there is some clear displacement of the central ridge in relation to the valleys either side. This is most obvious when comparing the change in shape of the dark shadow areas following correction. This is a good indication that the foreshortening effect is being corrected properly.

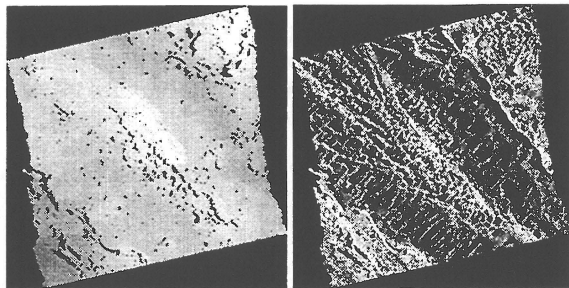


Figure 18. DEM (left) and Ortho Image (right) of Site 3.

A rendered 3-d view of the surface is shown in Figure 19 illustrates further the structure of the site and also shows more clearly the path carved by the river.

Profiles of the topography running North-South and West-East are shown in Figures 20 and Figure 21. Qualitatively, there is good agreement with the general trends in the topography along both profiles although there are some dramatic areas of disagreement, specifically on the backslopes of mountain ridges, where a more dramatic fall is seen in the DEM than in the map. This explains the missing backslope in to the left of Figure 20. To a lesser extent, this effect is also seen in the foreslopes.

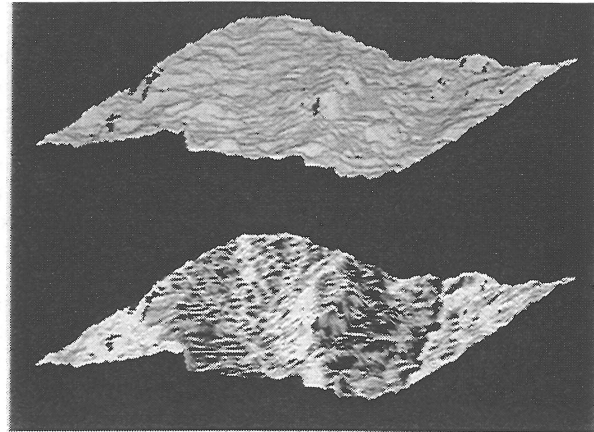


Figure 19. The DEM (top) and Image (bottom) viewed from the South West.

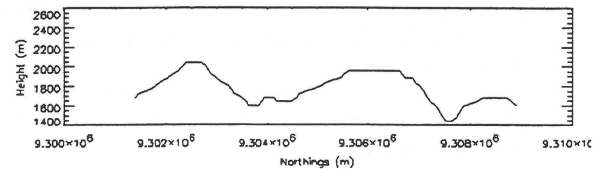
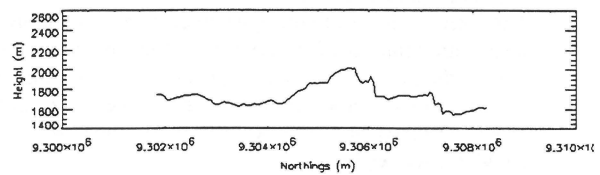


Figure 20. South-to-North Profiles from the Stereo-derived DEM (top) and the Maps (bottom)

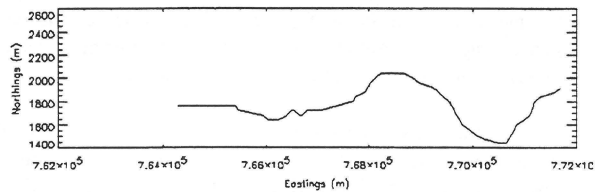
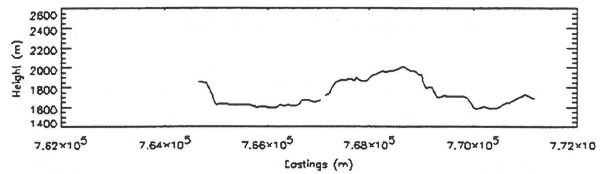


Figure 21. East-to-West Profiles from the Stereo-derived DEM (top) and the Maps (bottom)

In an area such as this, the stereo matcher has a great problem in areas susceptible to layover and shadow, as these areas tend to change their shape dramatically between the S7 and S2 images. Thus, we would expect a less accurate depiction of characteristics before and after a ridge from a profile. This is exactly what is seen. Still, the overall impression of the topography remains.

#### 4. COMPARISON OF RESULTS

The results of all three sites have been produced completely automatically with absolutely no ground control using a single command from the IDL tool prompt. The only manual intervention was to change over the image CD from the S7 to the S2 when prompted by the programme. Therefore, the results must be viewed in this context and, in all cases, the results are excellent. Specifically, the following observations were made during the analysis:

- All results showed general qualitative and quantitative agreement when profiles were drawn of the topography. This illustrates the generally good result of both the matching and the intersection processes, strengthened by the unique orbit correction applied in the software.
- The areas where the results were not so good were in areas having strong tendencies towards layover and shadow. This is to be expected as neither types of region allow any reasonable matching at all.
- The software is able to recognise such areas but simply fills them with some nominal value based on the mean values around the edges, which does not result in a pleasing result in most cases. However, interpolation over such areas is solely cosmetic and will not add to the accuracy of the DEM in such regions.
- Canyons are highlighted by the stereo analysis but, because of the extent of layover and shadow, are poorly described quantitatively. Height values for the canyon centre are usually too high.
- The positional accuracy of features was consistently high in all cases, meeting the error bounds on map and interpretation accuracy.

Probably, the main recommendation is to underline the detrimental effect of layover and shadow and, through selection of incidence angles and modes, to try to avoid them at all costs.

#### 5. CONCLUSIONS AND RECOMMENDATIONS

The results described above have shown conclusively that it is possible to derive low-cost topographic data from stereo SAR data. Furthermore, all data products shown were derived fully automatically, with no ground control or manual massaging of the results. Essentially, what is seen here is what is output by the process. This is an important observation, as the cost of generating such information is the most important factor in determining the commercial use of the method.

An accuracy assessment has been described above over three distinct areas of distinct terrain types. The results, in areas of low (Site 1) to moderate (Site 2) relief, are well within the limits of accuracy of the maps provided and the poor ground control points used. The poor ground control was due to the fact that the site had few features that correlated well with the maps apart from topographic features such as river canyons. As described, topographic features make for poor control but the relatively good results they give show the strength of the method. We would have no hesitation in stating that the results are perfectly acceptable as they are for producing topographic maps at scales between 1:50000 and 1:100000 over such areas.

For more mountainous areas (Site 3) the abundance of layover and shadow areas creates the greatest problem to any stereo

SAR methodology. Although the results were still good in terms of locational accuracy, the accurate description of backslopes and escarpments is problematic. For such areas, a different approach is necessary if high accuracy is still required. For such a case, Radarsat Fine Mode data may offer a solution as the angular range is less from F1 to F5 (38 - 47 degrees) than with S2 to S7 (27 - 47 degrees), reducing the overall layover effect. However, the problem of shadow still remains meaning that, for precise topographic mapping of mountainous areas, two side-looking fine mode pairs are recommended, one pair from ascending and one pair from descending passes, to cover both foreslopes and backslopes with precision. In this case two DEMs are generated automatically and combined to 'fill-in' the gaps in each other's coverage.

#### ACKNOWLEDGEMENTS

The work described was undertaken as part of a private venture project at the National Remote Sensing Centre Limited; the author is very grateful for the support and time granted him to complete the task. The Radarsat data was kindly made available to the project by Radarsat International.

#### REFERENCES

- Dowman, I., Twu, Z.-G. and Pu-Huai, C., 1997, "DEM Generation from Stereoscopic SAR", Proceedings of the First Radarsat Applications Symposium, Canada, April.
- ESA, 1997, "ENVISAT-1 Mission and System Summary", European Space Agency, March.
- Graham, L., 1980, "Stereo Radar for Mapping and Interpretation", in "Radar Geology: An Assessment, Report of the Radar Geology Workshop, Snowmass, Colorado, July 16-20, 1979", JPL Publication 80-61, September 1.
- Leberl, F., 1980, "Application of Imaging Radar to Mapping", in "Radar Geology: An Assessment, Report of the Radar Geology Workshop, Snowmass, Colorado, July 16-20, 1979", JPL Publication 80-61, September 1.
- MDA, 1995, "RADARSAT Canadian Data Processing Facility Product Specification CDRL No. IS-3", Ref: RZ-SP-50-5313, Issue 5, Revision 1, August 28.
- RSI, 1995, "RADARSAT Illuminated. Your Guide to Products and Services", Radarsat International Client Services, Canada.
- Toutin, T. and Carbonneau, Y., 1992, "MOS and SEASAT Image Geometric Corrections", IEE Trans. On Geoscience and Remote Sensing, Vol. 30, No. 3, May.